10-13-2019

A Dynamic Quantitative Microbial Risk Assessment for Norovirus in Potable Reuse System

Erfaneh Amoueyan
University of Nevada, Las Vegas

Sajjad Ahmad
University of Nevada, Las Vegas, sajjad.ahmad@unlv.edu

Joseph N.S. Eisenberg
University of Michigan

Daniel Gerrity
University of Nevada, Las Vegas, daniel.gerrity@unlv.edu

Microbial Risk Analysis xxx (xxxx) xxxx

Contents lists available at ScienceDirect

Microbial Risk Analysis

journal homepage: www.elsevier.com/locate/mran

Full length article

A dynamic quantitative microbial risk assessment for norovirus in potable reuse systems

Erfaneh Amoueyan[a,b], Sajjad Ahmad[a], Joseph N.S. Eisenberg[c], Daniel Gerrity[a,d,*]

[a] Department of Civil & Environmental Engineering and Construction, University of Nevada, Las Vegas, United States
[b] Jacobs Engineering Group, San Jose, California, United States
[c] Department of Epidemiology, School of Public Health, University of Michigan, Ann Arbor, MI, United States
[d] Applied Research and Development Center, Southern Nevada Water Authority, Las Vegas, NV, United States

ARTICLE INFO

Keywords:
Quantitative microbial risk assessment (QMRA)
Potable reuse
Norovirus
Dynamic disease transmission
Full advanced treatment (FAT)
Ozone

ABSTRACT

This study describes the results of a dynamic quantitative microbial risk assessment (QMRA) for norovirus (NoV) that was used to evaluate the relative significance of foodborne, person-to-person, and person-to-sewage-to-person transmission pathways. This last pathway was incorporated into simulated potable reuse systems to evaluate the adequacy of typical treatment trains, operational conditions, and regulatory frameworks. The results confirm that secondary and foodborne transmission dominate the overall risk calculation and that waterborne NoV likely contributes no appreciable public health risk, at least in the scenarios modeled in this study. *De facto* reuse with an environmental buffer storage time of at least 30 days was comparable or even superior to direct potable reuse (DPR) when compound failures during advanced treatment were considered in the model. Except during these low-probability failure events, DPR generally remained below the 10^{-4} annual risk benchmark for drinking water. Based on system feedback and the time-dependent pathogen load to the community's raw sewage, this model estimated median raw wastewater NoV concentrations of 10^{7}–10^{8} genome copies per liter (gc/L), which is consistent with high-end estimates in recent literature.

1. Introduction

Quantitative microbial risk assessments (QMRAs) for waterborne pathogens generally involve static models in which the probability of infection is calculated as a single exposure event with minimal (if any) time dependence or system feedback. This results in a disconnect between the number of shedding individuals at any given time, the pathogen load to the environment and the water/wastewater treatment infrastructure, and the implications for public health risk. This disconnect also makes it particularly difficult to fully characterize risks associated with highly contagious pathogens, such as norovirus (NoV), which often involve numerous 'secondary' infections (Zelner et al., 2010). Ultimately, static QMRAs may underestimate the true risk of waterborne disease within a community by not capturing the effects of secondary transmission. Conversely, static QMRAs can also overestimate the risk of waterborne disease by not accounting for its significance relative to other exposure pathways or its time dependence. Specifically, an individual exposed to a waterborne pathogen may become infected and diseased but may then enter a protected or immune state. The risk of developing a new infection during this epidemiological progression is diminished or negligible (Eisenberg et al., 2004).

In 1996, the International Life Sciences Institute (ILSI) collaborated with the United States (U.S.) Environmental Protection Agency (EPA) to develop a revised QMRA framework, specifically emphasizing the importance of secondary transmission and immunity in accurately characterizing certain pathogen risks (ILSI, 1996). Soon thereafter, Eisenberg et al. (1996) described the first dynamic model for waterborne disease and then expanded the model to account for the unique properties of target pathogens, including asymptomatic vs. symptomatic infection ratios; the duration of incubation, infection, and immunity; and shedding rate (Eisenberg et al., 2002, 2004). Fig. 1 illustrates these key properties and the principal epidemiological states, namely susceptible (S), exposed (E), carrier state 1 (C1), diseased (D), carrier state 2 (C2), and post-infection (P). There are now dynamic models that describe risk associated with recreational activities (Eisenberg et al., 1996), biosolids-amended soils (Eisenberg et al., 2004), the Milwaukee cryptosporidiosis outbreak (Eisenberg et al., 1998; Brookhart et al., 2002; Eisenberg et al., 2005), and the effects of post-infection immunity to NoV (Simmons et al., 2013). Although

* Corresponding author at: Applied Research and Development Center, Southern Nevada Water Authority, P.O. Box 99954, Las Vegas, NV 89193, United States.
E-mail address: daniel.gerrity@snwa.com (D. Gerrity).

https://doi.org/10.1016/j.mran.2019.100088
Received 24 June 2019; Received in revised form 3 October 2019; Accepted 12 October 2019

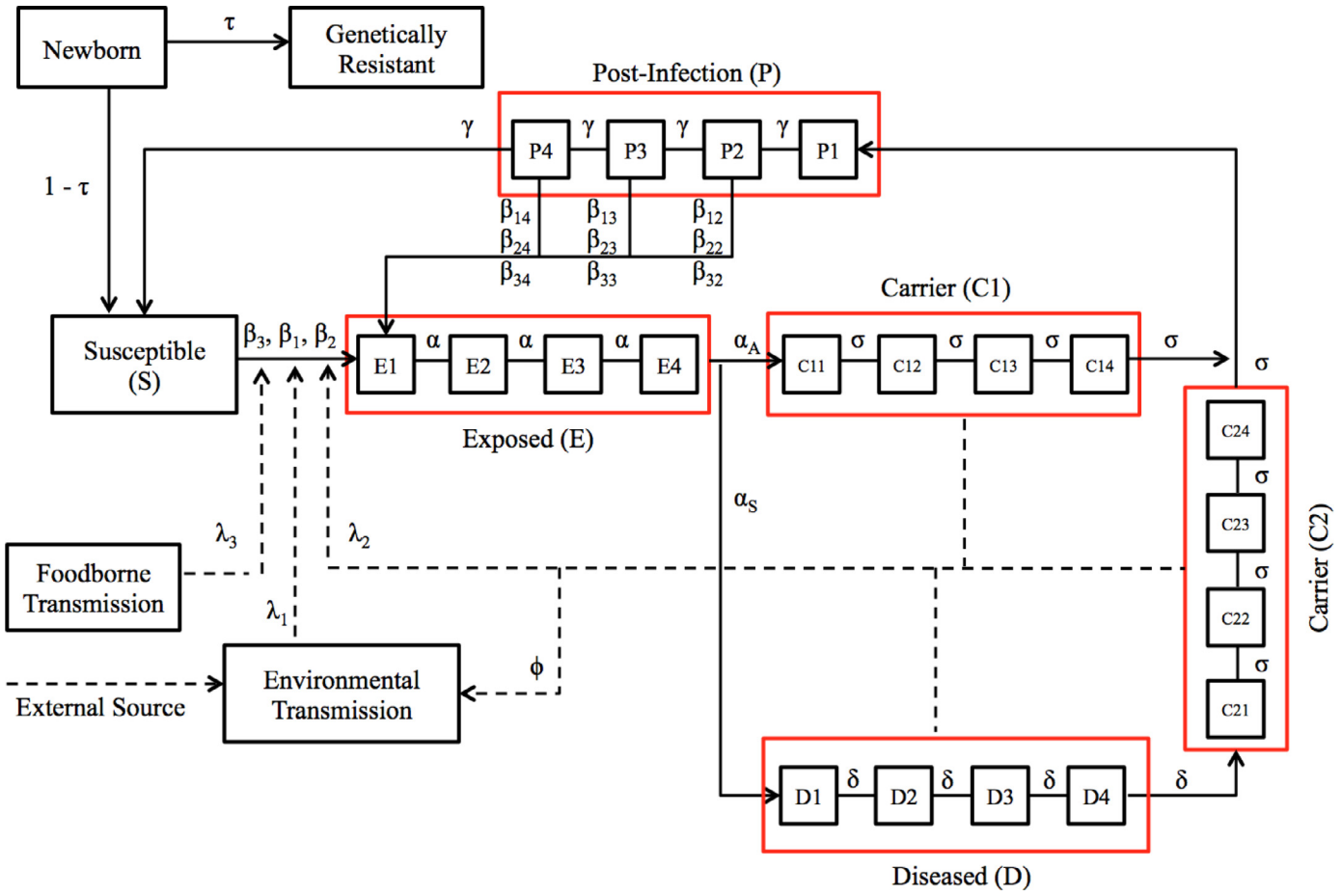

Fig. 1. Dynamic disease transmission model with 'distributed delays' used to simultaneously evaluate the impacts of primary and secondary transmission. A death rate was also incorporated into each epidemiological state but is not shown in the figure. The movement of individuals from one epidemiological state to another is represented with solid lines, and pathogen transmission routes are represented by dashed lines. Parameters/symbols are defined in Table 1.

Soller and Eisenberg (2008) confirmed that these dynamic models are warranted in high risk scenarios (i.e., >1 in 1,000), they also noted the difficulty in accurately defining some disease transmission parameters, thereby highlighting the potential suitability and preference for static models in some cases. Many static models can simultaneously address risks from a wide range of pathogens (Soller et al., 2017; Amoueyan et al., 2019), but this may be overly complex in dynamic models because of the varying epidemiology among bacterial, viral, and protozoan pathogens.

As noted earlier, NoV is a potential high risk pathogen warranting consideration for dynamic risk modeling. NoV is the most common cause of acute gastroenteritis in the U.S., with more than 20 million cases annually (Scallan et al., 2011; Hall et al., 2013). NoV is often transmitted through contaminated food, such as leafy green vegetables and fruit, with foodborne exposure accounting for more than 25% of all NoV-associated infections (Scallan et al., 2011) and up to 50% of all foodborne outbreaks in the U.S. (CDC, 2009, 2010, 2011). NoV has also been implicated in several outbreaks linked to contaminated wells or recreational water (Anderson et al., 2003; Parshionikar et al., 2003), and NoV has recently emerged as an important target pathogen for potable reuse.

Several studies have presented QMRAs for a wide variety of waterborne pathogens relevant to indirect potable reuse (IPR) and direct potable reuse (DPR) (Olivieri et al., 1999; Amoueyan et al., 2017, 2019; Chaudhry et al., 2017; Lim et al., 2017; Pecson et al., 2017; Soller et al., 2017), but recent studies have specifically implicated NoV as a potential driver of risk (Soller et al., 2017, 2018a,b). These existing models are based on static frameworks that do not account for the impacts of alternative exposure routes (e.g., consumption of contaminated food), secondary transmission, or the duration of post-infection immunity. Therefore, further study is needed to better characterize the relative risk of waterborne exposure to NoV in comparison with other exposure pathways (e.g., person-to-person or foodborne).

The objective of this study was to develop a dynamic QMRA to evaluate the risk of acquiring NoV-associated gastroenteritis in potable reuse systems, including the historically common practice of *de facto* reuse and also with DPR employing reverse osmosis or an ozone-based alternative treatment train. The resulting model incorporated treatment train reliability (i.e., nominal operating conditions vs. failure modes) and also a comparison of observed log removal values (LRVs) versus regulatory credits for advanced treatment processes. The dynamic nature of the model included the aforementioned epidemiological states and associated durations and allowed for system feedback. Specifically, the time-variant prevalence of infection/disease directly affected the pathogen load to the community's raw sewage. Primary exposure to NoV in drinking water was supplemented with secondary exposure to infected individuals within the community and primary exposure via contaminated food. Finally, the dynamic model allowed for a direct comparison with a corresponding static QMRA for NoV in potable reuse systems (Amoueyan et al., 2019).

2. Methodology

A conceptual comparison of a static QMRA and the current dynamic QMRA, which focuses on NoV as the primary hazard, is illustrated in Fig. 2. The dynamic QMRA assumed susceptible individuals could be

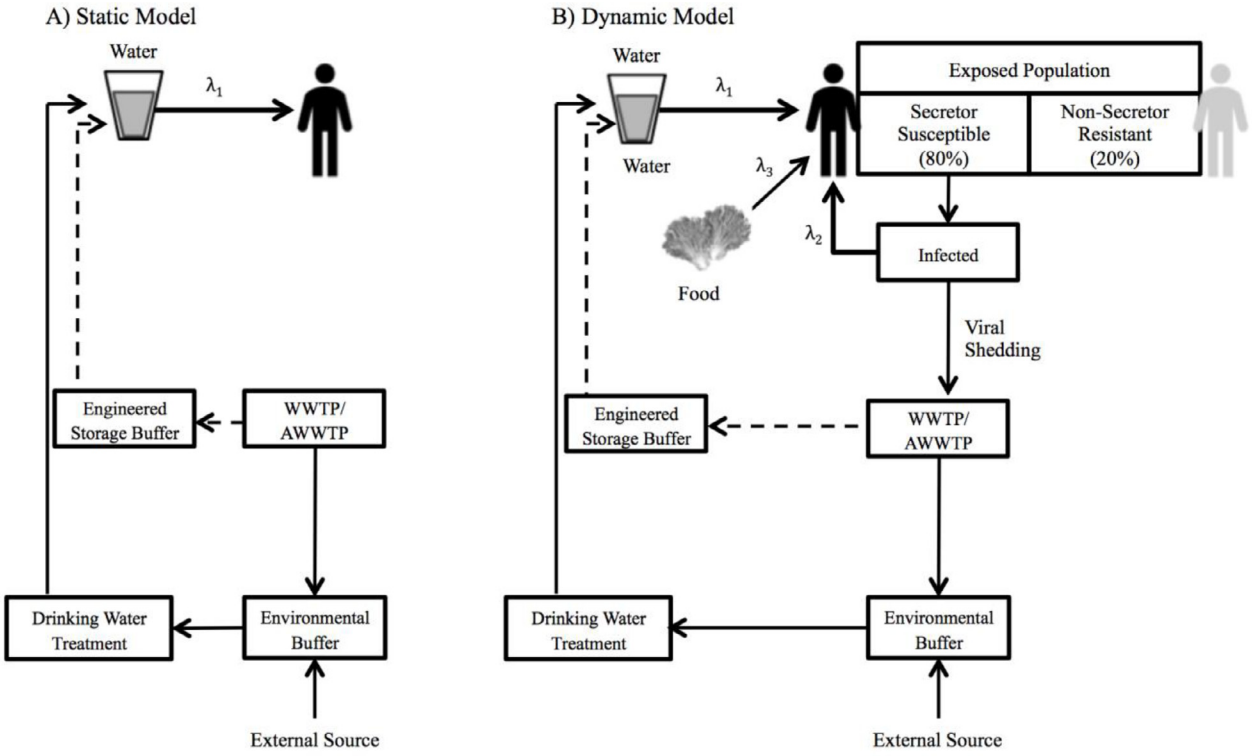

Fig. 2. Conceptual comparison of (A) static and (B) dynamic quantitative microbial risk assessment (QMRA) frameworks. The static framework represents the structure of the norovirus QMRA in Amoueyan et al. (2019), and the dynamic framework represents the structure of the current QMRA. Transmission rate constants (or forces of infection) are defined as follows: λ_1 = primary transmission rate constant for drinking water, λ_2 = secondary transmission rate constant, λ_3 = primary transmission rate constant for food. The solid lines represent travel of water through an IPR system, and dashed lines represent travel of water through a DPR system.

exposed to NoV through contaminated drinking water or food (i.e., primary transmission) or contact with infected individuals, surfaces, or fomites (i.e., secondary transmission) (Hall et al., 2012; Simmons et al., 2013; CDC, 2014). A Monte Carlo simulation platform was used to capture stochastic variability in certain model parameters (i.e., foodborne transmission rate constant, treatment process performance and failures, upstream surface water NoV concentration, duration within an epidemiological state, shedding rate, feces production rate, and wastewater generation rate) and under certain modeling scenarios (i.e., raw sewage NoV concentration for static modeling). For the dynamic configuration, the model simulated pathogen shedding into the wastewater to directly couple the prevalence of infection/disease within the community to drinking water risk. Each of these model components is described in greater detail in the following sections.

2.1. Norovirus epidemiology

The major components of NoV transmission and the corresponding assumptions used in the model are summarized in Fig. 1 and Table 1. The initial population of the community was set at one million and varied during the model simulation to account for births (rate constant = 3.4×10^{-5} day^{-1} or 3.4 births per 100,000) and deaths (rate constant = 2.3×10^{-5} day^{-1} or 2.3 deaths per 100,000) (NCHS, 2018). The birth rate was applied to the total population but only added individuals to the susceptible state, while the death rate was applied to all epidemiological states (S, E, C1, D, C2, and P). The initial latent population was assumed to be 0.056% of the total community (Scallan et al., 2011). Specifically, Scallan et al. (2011) estimated that there are ~5.5 million cases of foodborne NoV annually in the U.S. and that those cases account for ~26% of all symptomatic NoV infections. This results in a total of ~21 million symptomatic infections annually. Assuming a symptomatic ratio of 69% (Zhang et al., 2011; Teunis et al., 2015), there may be more than 30 million total NoV infections (symptomatic + asymptomatic) per year, which results in a total cumulative incidence of 0.103 infections/person-year assuming a total population of 299 million (Scallan et al., 2011). This annual cumulative incidence was then divided evenly over the year, which resulted in a cumulative incidence of 0.00056 infections/person (or 0.056% of the population) over a typical 2-day latency period (CDC, 2014).

Susceptibility to NoV is dependent upon the presence of histo-blood group antigens within the human gut, and fucosyltransferase 2 enzyme (FUT2) is required for secretion of these antigens. In non-secretors, inactivation of FUT2 prevents individuals from contracting an NoV infection (Currier et al., 2015; Nordgren et al., 2016). In the current study, non-secretors were assumed to comprise 20% of the initial population and 20% of births occurring during the model simulation (Currier et al., 2015; Simmons et al., 2013). Although these individuals were not at risk of developing or transmitting NoV infections, they were still considered in the overall population-based risk calculation. There were no further distinctions for sex, age, or immunocompromised individuals.

For the susceptible fraction of the population, the daily risk from drinking water (i.e., force of infection, λ_1) was calculated using the NoV concentration in the finished drinking water, an assumed water ingestion rate of 2 L/day (USEPA, 2004; WHO, 2008), and a fractional Poisson dose response model (Eq. (1); Messner et al., 2014).

$$P_{inf,d} = P \times (1 - e^{-\frac{Dose}{\mu}}) \quad (1)$$

where, $P_{inf,d}$ = daily probability of infection, P = fraction of susceptible subjects = 0.722 for NoV, Dose = number of NoV genome copies (gc) consumed, and μ = mean aggregate size = 1106 gc for NoV.

The average incubation period for NoV (i.e., duration from exposure to infection) was assumed to follow a uniform distribution ranging from 12 to 48 h (CDC, 2014), and the duration of disease was assumed to follow a uniform distribution ranging from 1 to 3 days (Aoki et al., 2010; CDC, 2014). The infected population was also divided into

Table 1
Summary of dynamic QMRA model parameters and values.

Parameter	Unit	Value	Reference
NoV shedding parameter			
Symptomatic individuals	gc/g-feces	Log_{10}uniform (8.2, 12.2)[a]	Atmar et al. (2008)
Asymptomatic individuals	gc/g-feces	Log_{10}uniform (7.5, 11.7)[a]	Atmar et al. (2008)
Feces production rate (ϕ)	g-feces/person-day	Uniform (200, 750)[a]	Rao (2006), Barker et al. (2013)
Wastewater generation rate	L/person-day	Uniform (189, 265)[a]	USEPA (2002)
Water ingestion rate	L/person-day	2.0	USEPA (2004), WHO (2008)
Initial population	persons	1,000,000	Assumed
Initial latent ratio	percent	0.056%	Scallan et al. (2011)
Birth rate constant	day^{-1}	3.4×10^{-5} (3.4 per 100,000)	NCHS (2018)
Death rate constant	day^{-1}	2.3×10^{-5} (2.3 per 100,000)	NCHS (2018)
Proportion of symptomatic infections	percent	69%	Zhang et al. (2011), Teunis et al. (2015)
Duration of latency ($1/\alpha$)	hours	Uniform (12, 48)[a]	CDC (2014)
Duration of disease ($1/\delta$)	days	Uniform (1, 3)[a]	Aoki et al. (2010), CDC (2014)
Duration of shedding ($1/\sigma$)	days	Uniform (2, 21)[a]	Atmar et al. (2008), Aoki et al. (2010)
Duration of immunity ($1/\gamma$)	years	Uniform (3.2, 5.1)[a]	Simmons et al. (2013)
Proportion of nonsecretors (τ)	percent	20%	Simmons et al. (2013), Currier et al. (2015)
λ_1 (waterborne transmission rate constant)	day^{-1}	Static or dynamic	Determined by model
λ_2 (secondary transmission rate constant)	day^{-1}	Dynamic	Model calibration (see Eq. (3))
λ_3 (foodborne transmission rate constant)	day^{-1}	Uniform (4.29×10^{-5}, 1.10×10^{-4})[a,c]	Scallan et al. (2011)
NoV dose response model (see Eq. (1))			
Fraction of susceptible subjects (P)	–	0.722	Messner et al. (2014)
Mean aggregate size (μ)	–	1106	Messner et al. (2014)
NoV occurrence			
WW (for static model)	gc/L	Lognormal (9.10, 2.56)[b]	Eftim et al. (2017) [n = 219]
SW (prior to blending)	gc/L	Lognormal (6.04, 1.22)[b]	Lodder and de Roda Husman (2005) [n = 8]
Environmental buffer			
SW recycled water contribution	percent	20%	Rice et al. (2015), Amoueyan et al. (2019)
SW storage time	days	270	Wu (2015), Amoueyan et al. (2019)
SW temperature	°C	20	Assumed
SW die-off rate constant	d^{-1}	0.862	Amoueyan et al. (2019)

[a] (minimum, maximum).
[b] (μ, σ) where $\mu = \ln(\frac{m^2}{\sqrt{s^2+m^2}})$, $\sigma^2 = \ln(1+\frac{s^2}{m^2})$, m = mean, s = standard deviation.
[c] adjusted to account for both symptomatic and asymptomatic foodborne infections.

symptomatic (69%) and asymptomatic (31%) infections (Zhang et al., 2011; Teunis et al., 2015). NoV shedding has been shown to be highly variable and has not been fully characterized (Atmar et al., 2008; Sabria et al., 2016) so log_{10}uniform distributions were used in this study to simulate shedding rate. Symptomatic individuals were assumed to shed 8.2 to 12.2 log_{10} gc/g feces, and asymptomatic individuals were assumed to shed 7.5 to 11.7 log_{10} gc/g feces. These values represent the estimated steady state and peak shedding rates, respectively, observed in 11 symptomatic and 5 asymptomatic infected individuals over a two-week observation period (Atmar et al., 2008). Studies have shown that shedding can last for 2 to 3 weeks post-infection (Okhuysen et al., 1995; Atmar et al., 2008), and post-symptomatic individuals (C2 in Fig. 1) sometimes shed at rates similar to when they were symptomatic (D in Fig. 1) (Milbrath et al., 2013). Therefore, the asymptomatic (C1) and post-symptomatic (C2) shedding periods were assumed to follow a uniform distribution ranging from 2 to 21 days with no change in shedding rate. The model assumed that all C1, D, and C2 individuals shed pathogens into the raw sewage. The feces production rate followed a uniform distribution ranging from 200 to 750 grams of feces per person-day (Rao, 2006; Barker et al., 2013), and wastewater generation rate followed a uniform distribution ranging from 189 to 265 liters per person-day for the entire community (USEPA, 2002).

The NoV post-infection period (i.e., duration of immunity) was originally suggested to be at least 6 months (Johnson et al., 1990), but Simmons et al. (2013) proposed a longer immunity period, which was incorporated into the current model as a uniform distribution ranging from 3.2 to 5.1 years. The acquired immunity that develops post-infection 'wanes' during the recovery period, in part due to NoV strain shift, until the individual returns to the fully susceptible state. To incorporate waning immunity, it was assumed that the level of protection during the immunity period ($1/\gamma$) decreased linearly from full protection to no protection (Eisenberg et al., 2004). Four different compartments with different levels of immunity were used to simulate the post-infection state (P1, P2, P3, and P4), with P1 representing full protection and P4 representing the least protection. Therefore, individuals in P2, P3, and P4 could theoretically move to the exposed state (E) through primary or secondary NoV exposure, or ultimately return to the susceptible state with no protection. Eq. (2) was used to define the rate constant (or force of infection) for movement from each P compartment to the exposed state (E) (Soller and Eisenberg, 2008).

$$\lambda_{ji} = \frac{\lambda_j(i - 1)}{n} \quad (2)$$

where, λ_{ji} = force of infection for post-infection state (d^{-1}); j = 1 (water) or 3 (food) for primary transmission or 2 for secondary transmission; i = 1, 2, 3, or 4 (depending on the protected state); and n = total number of compartments in the protected state = 4.

Secondary NoV transmission has been described as having a second-order rate constant (or force of infection) ranging from 0.08 to 0.24 secondary infections per shedding individual per day (Zelner et al. 2010). However, the Zelner et al. (2010) study of household NoV outbreaks noted that their secondary transmission model was not generalizable at the community or regional scale. Instead, the *de facto* reuse scenario in the current model (described later) was calibrated to match the aforementioned cumulative incidence of 0.103 infections/person-year (Scallan et al., 2011). The product of the calibrated parameter and the prevalence of shedding resulted in the pseudo first order rate constant (or force of infection, λ_2) shown in Eq. (3). No distinction was made for secondary transmission by symptomatic vs. asymptomatic individuals. The calibrated model parameter proved to be relatively consistent with the NoV secondary attack rate (14%–33%) reported in the literature (Karst et al., 2015).

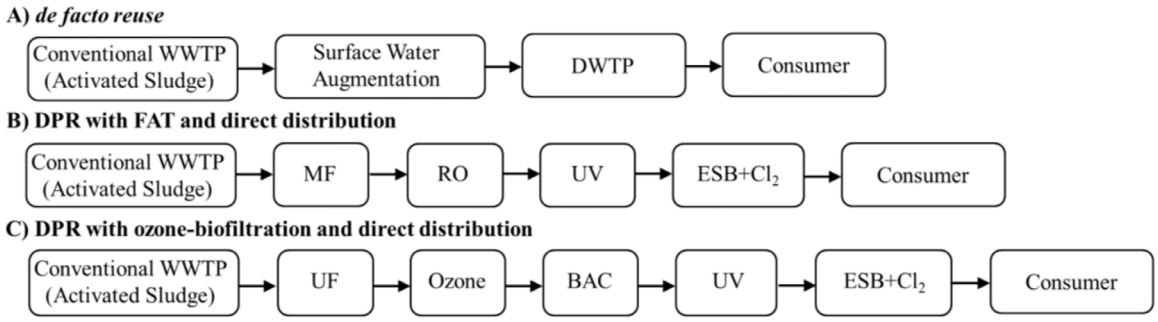

Fig. 3. Potable reuse treatment trains included in the dynamic QMRA. The conventional wastewater treatment plant (WWTP) included only secondary wastewater treatment. The drinking water treatment plant (DWTP) represented a conventional filtration system with chlorine (Cl_2) disinfection and was assumed to be compliant with the U.S. EPA's Surface Water Treatment Rules. The chlorination step included in the engineered storage buffer (ESB) was assumed to be compliant with guidelines for ESBs in DPR systems. DPR = direct potable reuse, FAT = full advanced treatment, MF = microfiltration, RO = reverse osmosis, UV = ultraviolet disinfection, UF = ultrafiltration, BAC = biological activated carbon.

$$\lambda_2 = 0.156 \times \frac{C1 + D + C2}{N} \quad (3)$$

where, λ_2 = time-variant secondary force of infection (day^{-1}); 0.156 = calibrated model parameter (day^{-1}); C1 + C2 + D = number of carrier/diseased individuals in the community (persons); and N = total population (persons).

Finally, the force of infection for primary transmission via contaminated food (λ_3) was incorporated into the model as a uniform distribution ranging from 4.29×10^{-5} day^{-1} to 1.10×10^{-4} day^{-1}. These values were determined from the 90% confidence interval for symptomatic foodborne NoV reported in Scallan et al. (2011), which ranged from 3.23 million to 8.31 million cases annually across a total population of 299 million. The values reported in Scallan et al. (2011) were increased to account for both symptomatic (69%) and asymptomatic (31%) infections.

2.2. Natural and engineered treatment processes

This QMRA focused on three different treatment scenarios: (a) *de facto* reuse, (b) direct potable reuse (DPR) with "full advanced treatment" (CDPH, 2014), and (c) DPR with ozone-based treatment (Fig. 3). Similar to Amoueyan et al. (2019), the current model simulated virus LRVs for dilution and natural die-off in the environmental buffer and inactivation and physical removal during engineered water and wastewater treatment. The 'observed' and 'regulatory' virus LRVs are summarized in Table 2 and are described in greater detail later. The current model assumed direct distribution to the consumer for the two DPR systems rather than raw water or treated water augmentation (i.e., blending before/after conventional drinking water treatment). The major distinction from Amoueyan et al. (2019) involved the dynamic nature of the model, which directly linked the prevalence of shedding in the community to pathogen loads in the raw sewage. For static scenario comparisons, the raw sewage was assumed to contain a lognormally distributed NoV concentration with μ = 9.10 and σ = 2.56 (Eftim et al., 2017; Table 1).

Each potable reuse system included a conventional wastewater treatment plant (WWTP), which was modeled with only secondary biological treatment and no disinfection. The 'observed' LRV for the WWTP was modeled as a normal distribution with a mean of 1.20 and standard deviation of 0.78 (distribution fit to data from Lodder and de Roda Husman, 2005), and the 'regulatory' LRV was modeled as a uniform distribution ranging from 1.0 to 2.0 (Trussell et al., 2016; SWRCB, 2016).

For the *de facto* reuse scenario, the treated wastewater was discharged to an environmental buffer (i.e., a surface water reservoir) with a baseline recycled water contribution (RWC) of 20% (Rice et al., 2015; Amoueyan et al., 2019) and a baseline storage time of 270 days (Wu, 2015; Amoueyan et al., 2019). Sensitivity analyses for *de facto* reuse included an RWC of 1% and storage times of 0, 15, and 30 days. Die-off of wastewater-derived NoV was calculated using a first-order, base *e* rate constant of 0.862 d^{-1} (Amoueyan et al., 2019), which is consistent with the rate constant reported for murine NoV in a recent meta-analysis (Boehm et al., 2018). The corresponding LRVs as a function of storage/travel time are summarized in Fig. S1 in the Supplementary Information (SI). The model assumed the treated wastewater was blended with an upstream surface water (not impacted by storage/travel time) containing a lognormally distributed NoV concentration with μ = 6.04 and σ = 1.22 (distribution fit to data from Lodder and de Roda Husman, 2005; Table 1).

Table 2
Pathogen log reduction values (LRVs) for engineered treatment processes. A temperature of 25 °C was assumed for ozone CT calculations. Failure probabilities reflected the production of a random 2-L aliquot of water each day. N = normal distribution (mean, standard deviation) and U = uniform distribution (min, max).

Process	Failure Probability	Observed LRVs	Regulatory LRVs
WWTP CAS	–	N (1.20, 0.78)[c]	U (1.0, 2.0)[m,n]
DWTP filter	0.0[a]	2.0[d]	2.0[d]
DWTP Cl_2	0.0[a]	4.0[e]	4.0[e]
MF	0.0029[b]	U (1.50, 3.30)[f]	0.0[m,n]
UF	0.0029[b]	N (4.00, 0.10)[g,h]	1.0[m,n]
RO	0.018[a]	N (4.30, 0.34)[g,i]	U (1.0, 2.0)[m,n]
BAC	0.0[a]	U (0.00, 1.00)[f]	0.0[m,n]
Ozone	0.0022[b]	Determined based on ozone CT (Eq. (4)); Baseline CT = 5 mg-min/L [j,k]	
UV	0.002[a]	Determined based on UV dose (Eq. (5)); Baseline UV dose = 80 mJ/cm^2 [j,k]	
ESB Cl_2	0.0[a]	4.0[l]	4.0[l]

[a] Soller et al. (2018b).
[b] Forss and Ander (2011).
[c] Lodder and de Roda Husman (2005).
[d] USEPA (2006).
[e] Regli et al. (1991).
[f] Soller et al. (2017).
[g] Chaudhry et al. (2017).
[h] Matsushita et al. (2013).
[i] Governal and Gerba (1999) with MS2 as a surrogate.
[j] Amoueyan et al. (2017).
[k] Text S2.
[l] Salveson et al. (2016).
[m] Trussell et al. (2016).
[n] SWRCB (2016). WWTP = wastewater treatment plant; CAS = conventional activated sludge; DWTP = drinking water treatment plant; Cl_2 = chlorine disinfection; MF = microfiltration; UF = ultrafiltration; RO = reverse osmosis; BAC = biological activated carbon; UV = ultraviolet disinfection; ESB = engineered storage buffer.

For *de facto* reuse, the blended water was then treated at a conventional drinking water treatment plant (DWTP), which was credited with 2.0 logs for filtration [consistent with the U.S. EPA's Surface Water Treatment Rule (SWTR)] and an additional 4.0 logs for chlorine disinfection. According to Regli et al. (1991), a chlorine CT achieving 0.5-log removal/inactivation of *Giardia*, which would meet the requirements of the U.S. EPA's SWTR, would also achieve >4-log virus inactivation, hence the 4-log credit for chlorine disinfection at the DWTP.

The DPR system with full advanced treatment (FAT) included a conventional WWTP, microfiltration (MF), reverse osmosis (RO), ultraviolet (UV) disinfection, an engineered storage buffer with free chlorine disinfection, and direct distribution to the consumer. The combination of RO and a UV advanced oxidation process (AOP) is described as FAT in some regulatory contexts (Gerrity et al., 2013; CDPH, 2014). The UV process in the current study was modeled with a more conservative disinfection-based dose of 80 mJ/cm^2 instead of the higher doses typically employed for AOPs (i.e., >100 mJ/cm^2). The ozone-based DPR system included a conventional WWTP, ultrafiltration (UF), ozone, biological activated carbon (BAC), UV disinfection, an engineered storage buffer with free chlorine disinfection, and direct distribution to the consumer.

For DPR, pathogen attenuation was modeled with point estimates, probability distributions based on observed performance or typical regulatory credits, or a calculated value based on conditions simulated by the model (for ozone and UV) (Table 2). The ozone LRV was calculated using Eq. (4), which is a generalized ozone dose response curve for virus inactivation (USEPA, 2010), and an assumed temperature during treatment of 25 °C. The target ozone CT was 5 mg-min/L, but the actual CT was calculated by the model based on ozone demand/decay kinetics (Amoueyan et al., 2017) and simulated water quality (described later).

$$-\log\left(\frac{N}{N_0}\right) = 2.1744 \times (1.0726)^{Temp} \times CT \quad (4)$$

where, CT = product of ozone residual and contact time (mg-min/L) and Temp = temperature (°C). The LRV for UV disinfection was calculated using Eq. (5) and a base 10 rate constant of 0.150 (mJ/cm^2)$^{-1}$, which is based on experiments with murine norovirus (Lee et al., 2008).

$$-\log\left(\frac{N}{N_0}\right) = k_{UV} \times D \quad (5)$$

where, k_{UV} = base 10 UV_{254} inactivation rate constant = 0.150 (mJ/cm^2)$^{-1}$ and D = UV_{254} dose (mJ/cm^2).

In accordance with CDPH (2014), the model LRVs for ozone and UV were limited to 6.0 logs for both the 'observed' and 'regulatory' scenarios. The 'regulatory' scenario was most impacted by changes in membrane LRVs, with MF receiving 0 logs, UF limited to 1.0 log (point estimate), and RO limited to a uniform distribution ranging from 1.0 to 2.0 logs (Trussell et al., 2016; SWRCB, 2016).

Treatment train performance considered unit process failures (modeled with an LRV of 0) using published failure probabilities (Forss and Ander, 2011; Soller et al., 2018b; Table 2), and the model also considered cascading failures or 'domino effects'. As described previously in Amoueyan et al. (2019), both DPR systems assumed a baseline UV dose of 80 mJ/cm^2, and the ozone-based DPR system assumed a baseline ozone to total organic carbon ratio (O_3/TOC) of 1.1 during nominal operating conditions, which achieved an ozone CT of 5 mg-min/L. Failures of one or more upstream treatment processes resulted in increases in TOC concentration and the UV_{254} absorbance of the target water matrix (Amoueyan et al., 2017; 2019), as summarized in Table S2. The model assumed the applied ozone dose, ozone contact time, incident UV intensity, and UV exposure time all remained constant during a cascading failure condition, thereby reducing the efficacy of these processes due to the change in feed water quality (Text S2). The resulting LRVs for ozone and UV are summarized in Tables S3 and S4. Because of the assumed robustness of ozone and UV for NoV inactivation, the only cascading failures that actually impacted performance were simultaneous failures of MF and RO (LRV = 4.1 for UV) and UF and ozone (LRV = 4.2 for UV). All other scenarios resulted in the maximum allowable LRV of 6.0 for ozone and/or UV, except when those specific processes failed and were credited with 0 logs.

2.3. Model scenarios

Model simulations were performed for multiple scenarios to elucidate the relative significance of each exposure pathway. For scenario 1, exposure to NoV occurred only through contaminated drinking water, and the corresponding pathogen load to the wastewater treatment plant was dynamic in nature due to infected individuals shedding NoV into the raw sewage (λ_1 = dynamic, λ_2 = 0, λ_3 = 0). For scenario 2, exposure to NoV occurred through contaminated drinking water, secondary transmission, and contaminated food (λ_1 = dynamic, λ_2 = dynamic, λ_3 = uniform distribution); scenario 2 also included a comparison of 'observed' vs. 'regulatory' LRVs for the DPR systems. For scenario 3, exposure to NoV occurred through contaminated drinking water, secondary transmission, and contaminated food, but the raw sewage pathogen load was static in nature (λ_1 = static, λ_2 = dynamic, λ_3 = uniform distribution). Finally, scenarios 4 and 5 included a dynamic drinking water risk, but only secondary transmission (scenario 4: λ_1 = dynamic, λ_2 = dynamic, λ_3 = 0) or foodborne transmission (scenario 5: λ_1 = dynamic, λ_2 = 0, λ_3 = uniform distribution) was included as an alternative exposure route. These scenarios are summarized later in Table 3.

2.4. Modeling approach and risk calculations

The dynamic model was developed in STELLA 10.1 (ISEE Systems, Lebanon, NH). The movement of individuals through the various epidemiological states was modeled using a series of ordinary differential equations based on the model structure illustrated in Fig. 1 and the parameters summarized in Table 1. All states except the susceptible state (S) were modeled as distributed delays using gamma distributions with a shape parameter of 4 (Soller and Eisenberg, 2008; Zelner et al., 2010; Fig. 1). Because the model simulated true travel times for each 'parcel' of water and for movement of individuals between epidemiological states, a typical 365-day simulation would not have been adequate to achieve steady state conditions (Eisenberg et al., 2004). Instead, each model iteration included daily estimates over a 10-year simulation (3650 data points per iteration), and overall results were based on 1,000 model iterations (3,650,000 total data points). A 'delta time' (DT) value (i.e., the time interval simulated by each model calculation) was set at 1/8th of a day in the STELLA 10.1 software.

Daily cumulative incidence (CI_{daily}) was used as the principal measure of overall risk and was calculated as the number of individuals who entered either the diseased state (D) or the asymptomatic carrier state (C_1) during each simulated day divided by the total population for that day (Eisenberg et al., 2004; Soller and Eisenberg, 2008). The CI was then annualized for each simulation year (i.e., 10 CI_{annual} values per iteration) using Eq. (6). Therefore, CI_{annual} can also be described as the annual risk of infection per person for the dynamic QMRA.

$$CI_{annual} = 1 - \prod_{i=1}^{365} (1 - CI_{daily})_i \quad (6)$$

where, CI_{annual} = cumulative incidence for a given simulation year (infections/person-year) and CI_{daily} = daily cumulative incidence (infections/person-day).

The model was validated as suggested by Sterman (2000). These tests included structure assessment, dimensional consistency, behavior reproduction, integration error, extreme conditions, and sensitivity analysis. Moreover, results from the previous static model

Table 3
Annual cumulative incidence (CI_{annual}; infections/person-year) over the 10-year simulation period as a function of potable reuse paradigm, treatment train, and modeling scenario. For the 'static' conditions, the drinking water risk (λ_1) was determined using statistical distributions of NoV concentration in the raw sewage and upstream surface water (when applicable) and attenuation during engineered treatment and in the environmental buffer (EB; when applicable). For the 'dynamic' conditions, the NoV concentration in the raw sewage was directly linked to pathogen shedding within the community. λ_2 (secondary transmission) and λ_3 (foodborne transmission) are defined in Table 1. For DPR, scenario 2 was modeled with (a) observed and (b) regulatory log removal values for each engineered treatment process (see Table 2).

Model	λ_1	λ_2	λ_3	Mean	SD	50th	95th	Max
***de facto*: WWTP-EB-DWTP**								
Static[a]	Static	0	0	3.39×10^{-4}	3.14×10^{-5}	3.36×10^{-4}	3.95×10^{-4}	4.86×10^{-4}
Dynamic 1	Dynamic	0	0	2.81×10^{-4}	3.36×10^{-5}	2.71×10^{-4}	3.76×10^{-4}	4.12×10^{-4}
Dynamic 2	Dynamic	Dynamic	Uniform	1.03×10^{-1}	4.98×10^{-2}	8.63×10^{-2}	2.51×10^{-1}	2.52×10^{-1}
Dynamic 3	Static	Dynamic	Uniform	1.03×10^{-1}	4.98×10^{-2}	8.63×10^{-2}	2.51×10^{-1}	2.52×10^{-1}
Dynamic 4	Dynamic	Dynamic	0	5.18×10^{-2}	5.70×10^{-2}	3.08×10^{-2}	1.89×10^{-1}	1.89×10^{-1}
Dynamic 5	Dynamic	0	Uniform	2.11×10^{-2}	4.30×10^{-4}	2.10×10^{-2}	2.21×10^{-2}	2.24×10^{-2}
DPR1: WWTP-MF-RO-UV-ESB (Scenario 2a = observed LRVs and Scenario 2b = regulatory LRVs)								
Static[a]	Static	0	0	1.45×10^{-8}	2.19×10^{-7}	4.40×10^{-11}	5.31×10^{-9}	5.01×10^{-6}
Dynamic 1	Dynamic	0	0	N/A	N/A	N/A	N/A	N/A
Dynamic 2a	Dynamic	Dynamic	Uniform	1.03×10^{-1}	5.04×10^{-2}	8.60×10^{-2}	2.51×10^{-1}	3.47×10^{-1}
Dynamic 2b	Dynamic	Dynamic	Uniform	1.28×10^{-1}	7.83×10^{-2}	9.91×10^{-2}	3.08×10^{-1}	4.62×10^{-1}
Dynamic 3	Static	Dynamic	Uniform	1.02×10^{-1}	4.98×10^{-2}	8.60×10^{-2}	2.51×10^{-1}	2.51×10^{-1}
Dynamic 4	Dynamic	Dynamic	0	4.88×10^{-2}	5.86×10^{-2}	8.17×10^{-3}	1.87×10^{-1}	3.22×10^{-1}
Dynamic 5	Dynamic	0	Uniform	2.09×10^{-2}	1.51×10^{-3}	2.08×10^{-2}	2.18×10^{-2}	8.65×10^{-2}
DPR2: WWTP-UF-O3-BAC-UV-ESB (Scenario 2a = observed LRVs and Scenario 2b = regulatory LRVs)								
Static[a]	Static	0	0	1.68×10^{-11}	5.21×10^{-10}	0.00	5.18×10^{-13}	1.65×10^{-8}
Dynamic 1	Dynamic	0	0	N/A	N/A	N/A	N/A	N/A
Dynamic 2a	Dynamic	Dynamic	Uniform	1.02×10^{-1}	4.98×10^{-2}	8.59×10^{-2}	2.51×10^{-1}	2.52×10^{-1}
Dynamic 2b	Dynamic	Dynamic	Uniform	1.03×10^{-1}	4.99×10^{-2}	8.59×10^{-2}	2.51×10^{-1}	2.88×10^{-1}
Dynamic 3	Static	Dynamic	Uniform	1.02×10^{-1}	4.98×10^{-2}	8.60×10^{-2}	2.51×10^{-1}	2.51×10^{-1}
Dynamic 4	Dynamic	Dynamic	0	4.87×10^{-2}	5.76×10^{-2}	2.47×10^{-2}	1.87×10^{-1}	1.88×10^{-1}
Dynamic 5	Dynamic	0	Uniform	2.08×10^{-2}	4.22×10^{-4}	2.08×10^{-2}	2.18×10^{-2}	2.22×10^{-2}

[a] Amoueyan et al. (2019).

(Amoueyan et al., 2019) were compared with the current dynamic model to evaluate consistencies/differences in model output.

3. Results and discussion

3.1. Annual cumulative incidence

Table 3 summarizes the annualized cumulative incidence for each of the potable reuse systems and modeling scenarios. For *de facto* reuse, a comparison of the static model (Amoueyan et al., 2019) and scenario 1 provides validation for the dynamic modeling framework in that the various CI_{annual} values were relatively consistent between each study. As noted in Amoueyan et al. (2019) and explained later, wastewater-derived NoV had no discernible impact on annual risk in the *de facto* reuse system because of the robustness of the environmental buffer. Therefore, the lower CI_{annual} observed for the dynamic model resulted from the time dependence of the epidemiological states, particularly the duration of immunity. In both models, the mean and median CI_{annual} was approximately 3×10^{-4} infections/person-year, again dominated by the upstream surface water NoV concentration, and the maximum CI_{annual} was approximately 4×10^{-4} infections/person-year for the dynamic model and 5×10^{-4} infections/person-year for the static model.

For *de facto* reuse, scenarios 2 (dynamic $\lambda_1+\lambda_2+\lambda_3$) and 3 (static $\lambda_1+\lambda_2+\lambda_3$) resulted in identical CI_{annual} values because the risk was dominated by secondary and foodborne transmission. The effects of pathogen shedding into the raw wastewater were negated by the dominance of the alternative exposure pathways and the robustness of the environmental buffer, which attenuated any increase in raw sewage NoV concentrations. In scenario 4, the mean CI_{annual} decreased by approximately 50% once foodborne transmission was eliminated, while in scenario 5, the elimination of secondary transmission resulted in an 80% reduction in CI_{annual}. Therefore, the model demonstrated that secondary transmission was the most important exposure pathway, which is consistent with NoV epidemiology.

The DPR results were generally identical to those of the *de facto* reuse system for scenarios 2a and 3, which is expected considering that secondary transmission and primary transmission via contaminated food were the dominant exposure pathways. The robustness of the DPR treatment trains with 'observed' LRVs generally masked differences in raw sewage pathogen loading for the dynamic (scenario 2a) and static (scenario 3) scenarios. The only exception was the maximum risk for FAT-based DPR, which was slightly higher for the dynamic pathogen loading in scenario 2a. In fact, it was not even possible to run scenario 1 for DPR (dynamic λ_1 and $\lambda_2 = \lambda_3 = 0$) because the DPR systems adequately attenuated the NoV shed by the initial latent population, and there were no further inputs of NoV into the system. Scenario 2b ('regulatory' LRVs) exhibited a 13% increase in the maximum CI_{annual} for ozone-based DPR and increases of 15–33% for all risk estimates for FAT-based DPR. Therefore, even with 'regulatory' LRVs, ozone-based DPR was sufficiently robust to attenuate all pathogen loads, except in the case of a low-frequency compound failure (i.e., maximum risk). FAT-based DPR was more sensitive to the lower 'regulatory' LRVs, and the adverse effects were not limited to compound failure instances.

To evaluate potential links between maximum risk and time, maximum CI_{annual} was plotted as a function of simulation year, with the results for *de facto* reuse presented in Fig. 4 and DPR presented in Fig. S2. Year 1 exhibited the highest CI_{annual} for most systems and modeling scenarios, in part due to the initial latent population. For *de facto* reuse under scenario 1, the risk decreased from the year 1 max and rapidly reached steady state at a slightly lower value than estimated by the static model. With the effects of secondary and foodborne transmission (scenarios 2 and 3), similar temporal trends were observed for all three potable reuse systems, although the risks were elevated and consistent with the aforementioned data from Table 3. The most interesting temporal trend was observed for scenario 4, which was dominated by secondary transmission in the absence of foodborne transmission ($\lambda_3 = 0$). This combination caused a significant oscillation in maximum CI_{annual}, which fluctuated by several orders of magnitude for the first several years. The data exhibited a dampening effect toward the end of

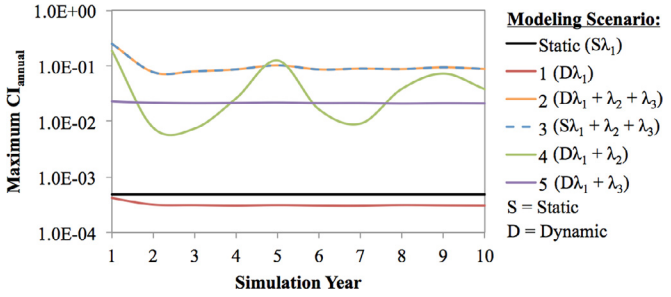

Fig. 4. Maximum annual cumulative incidence (infections/person-year) for the *de facto* reuse system as a function of simulation year and static and dynamic modeling scenarios. The data represent the maximum values for each simulation year across 1000 model simulations, except for the static scenario. The corresponding data for direct potable reuse are provided in Fig. S2.

the simulation, as the maximum CI_{annual} for each potable reuse system approached that of scenario 2(a). Scenario 5 ($\lambda_2 = 0$) was dominated by foodborne transmission, for which the corresponding rate constant was modeled as a uniform distribution, so it exhibited little variability in maximum CI_{annual} across the 10-year simulation.

3.2. Isolating the effects of treatment on drinking water risk

3.2.1. Log removal value distributions

While the model and actual epidemiology of NoV agree that alternative exposure routes appear to dominate public health risk, it is still important to understand how the level of treatment in a potable reuse system specifically impacts drinking water risk. Fig. 5 illustrates the distribution of LRVs for *de facto* reuse (with and without an environmental buffer), FAT-based DPR, and ozone-based DPR. The corresponding frequency distributions and raw data for Fig. 5 are shown in Fig. S3. Because the baseline storage time of 270 days resulted in an equivalent LRV of ~100, results for shorter storage times of 0, 15, and 30 days are provided in Figs. 5 and S3.

These results indicate that *de facto* reuse with a storage time of at least 15 days or DPR with either 'regulatory' or 'observed' LRVs is generally sufficient to achieve the 12-log benchmark for virus removal. *De facto* reuse with 15-day storage was comparable to FAT-based DPR, while *de facto* reuse with 30-day storage was comparable to ozone-based DPR. The LRV sometimes dropped below the 12-log benchmark during failure conditions, with absolute minimum LRVs of 5.0 for 'regulatory' FAT, 5.5 for 'observed' FAT, 6.1 for 'regulatory' ozone, and 6.4 for 'observed' ozone-based treatment (Fig. 5). These extreme conditions are highly improbable (i.e., <20 instances per 3,650,000 data points) because they require compound treatment failures (e.g., simultaneous failures of O_3 and UV for ozone-based DPR) in addition to low estimates for the remaining treatment processes (e.g., activated sludge and BAC). Moreover, as noted in Amoueyan et al. (2019), the framework in the current model may provide reasonable estimates of failure frequency but may overestimate the severity of a failure, as compound treatment failures resulting in actual LRV reductions may have probabilities as low as 10^{-11} (Pecson et al., 2018). Therefore, all potable reuse systems in the current study are expected to consistently achieve the 12-log benchmark for virus removal/inactivation. The *de facto* reuse system with at least 30-day storage, FAT-based DPR with 'observed' credits, and ozone-based DPR also achieve the 15-log target recommended by Soller et al. (2018a).

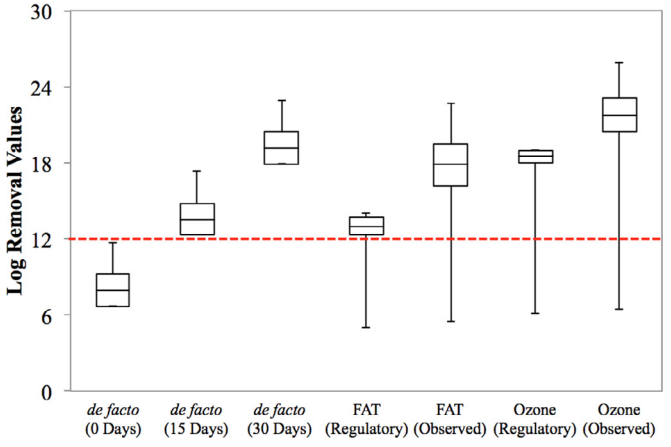

Fig. 5. Model output for log removal values (LRVs), with distributions demonstrating the implications of treatment process variability and failure. The *de facto* reuse data indicate the cumulative LRV for the engineered treatment processes, dilution, and die-off for the indicated storage time. The baseline condition for the environmental buffer was actually 270 days, which resulted in an equivalent LRV of ~100. For full advanced treatment (FAT) and ozone-based direct potable reuse (DPR), separate data are shown for typical regulatory LRVs and observed LRVs from the literature. Boxes represent 5th, 50th, and 95th percentiles, and whiskers indicate minimum and maximum values. The dashed line represents the target LRV for virus inactivation and removal in some U.S. potable reuse regulations.

3.2.2. *de facto* reuse assuming 'pristine' upstream surface water

To isolate the effects of wastewater-derived NoV on *de facto* reuse, the NoV contribution from the upstream surface water was eliminated, and the model was also revised to include RWCs of 1% and 20% and storage times of 0, 15, and 30 days. The resulting daily drinking water risks (dynamic λ_1) and daily cumulative incidences (CI_{daily}; also includes effects of λ_2 and λ_3) are illustrated in Fig. 6. As expected, there were clear increases in λ_1 with shorter storage times and with the higher RWC of 20%, but assuming at least 15 days of storage, there was no difference in CI_{daily} for RWCs of 1% or 20%, thereby indicating that the alternative exposure routes were still dominating the overall risk. This is consistent with the high LRV achieved by *de facto* reuse with at least 15 days of storage (Fig. 5).

With 0 days of storage, which effectively represented a DPR scenario, there was a sufficient increase in λ_1 to cause a noticeable change in CI_{daily}. In fact, because λ_1 was so high, it caused a sharp spike in infections within the community early in the simulation, which was then followed by a sharp decline in infections due to the lower population of susceptible individuals, particularly for the RWC of 1%. This is reflected in the wide distribution of λ_1 and CI_{daily} values for 0-day storage in Fig. 6. The time dependencies of λ_1 and CI_{daily} are also illustrated in Fig. 7. For 0-day storage, RWCs of 1% and 20% both resulted in a similar CI_{daily}, but the RWC of 1% fluctuated more throughout the simulation. With low drinking water risk (i.e., storage time ≥15 days), there was a small spike in CI_{daily} early in the simulation, which was actually unrelated to drinking water risk, and then CI_{daily} quickly reached a steady state condition.

According to Brunkard et al. (2011), only 6.4% of all waterborne disease cases associated with drinking water in the U.S. between 2007 and 2008 (265 out of 4,128 cases) were linked to NoV. Assuming a symptomatic ratio of 69%, this would yield a total of 384 infections across ~300 million people. This corresponds with an estimated annual NoV risk from drinking water of 1.3×10^{-6}, or a daily NoV risk from drinking water of $\lambda_1 = 3.5 \times 10^{-9}$. According to Fig. 7, this is consistent with the estimated drinking water risk for *de facto* reuse with 15 days of storage and an RWC of 1%, which suggests that this combination might be broadly representative of drinking water systems in the U.S.

3.2.3. Direct potable reuse

The distributions in daily drinking water risk (λ_1) for the DPR systems are illustrated in Fig. 8. The distributions differed considerably between the various modeling scenarios for several reasons, including the effects of FAT vs. ozone-based treatment, 'observed' vs. 'regulatory'

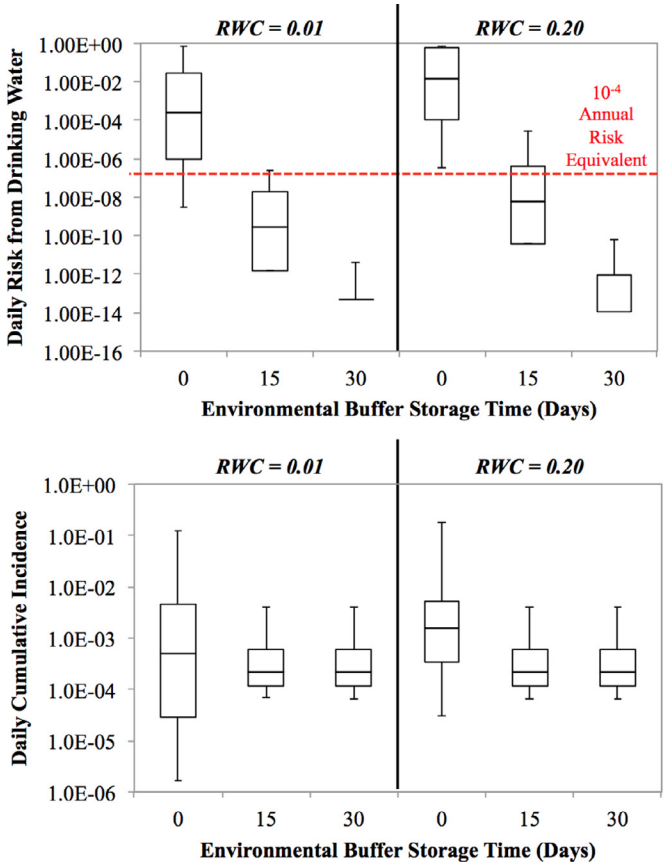

Fig. 6. (top) Daily risk from drinking water (λ_1, d^{-1}) and (bottom) daily cumulative incidence (CI_{daily}, infections/person-day) as a function of environmental buffer storage time in *de facto* reuse systems. These model output assumed no NoV were present in the upstream surface water to isolate the effects of wastewater-derived NoV. Daily cumulative incidence included contributions from secondary and foodborne transmission. For each graph, separate plots are shown for recycled water contributions (RWCs) of (left) 0.01 and (right) 0.20. Boxes represent 5th, 50th, and 95th percentiles, and whiskers indicate minimum and maximum values. The dashed line in the top figure corresponds to an annualized risk of 10^{-4}.

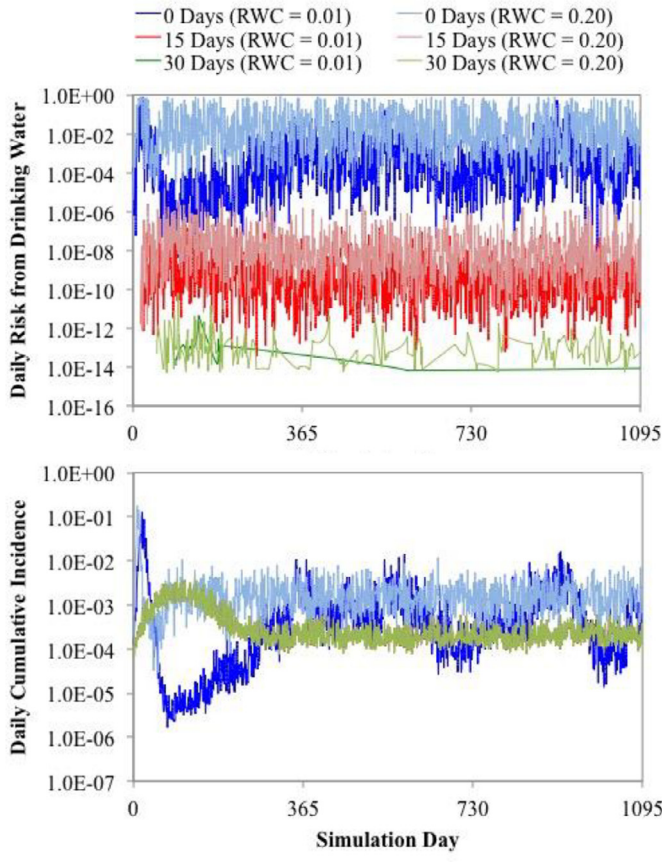

Fig. 7. Temporal variability in (top) daily drinking water risk (λ_1, d^{-1}) and (bottom) daily cumulative incidence (CI_{daily}, infections/person-day) for the *de facto* reuse system as a function of environmental buffer storage time and recycled water contribution (RWC). For CI_{daily}, all 15-day and 30-day data overlap. The model output assumed no NoV were present in the upstream surface water to isolate the effects of wastewater-derived NoV. Daily cumulative incidence included contributions from secondary and foodborne transmission.

LRVs, dynamic vs. static λ_1, and whether alternative exposure pathways (λ_2 and λ_3) were considered. For all scenarios except 'regulatory' FAT (i.e., scenario 2b), the 95th percentile risk was lower than the 10^{-4} annual risk equivalent, but the maximum risks exceeded that benchmark. As explained earlier, this was due to infrequent compound failures causing significant reductions in the overall LRV for each DPR treatment train. In some cases, particularly for ozone-based DPR, the maximum risk was the only value that could be calculated by the model because all other risk estimates were ~0.

For scenario 3 (static λ_1), only the 95th percentile and/or maximum risk could be calculated by the model for both DPR treatment trains. This indicated that the pathogen load to the wastewater treatment plant under static conditions was more easily attenuated during treatment. As shown in Fig. 9, the lognormally distributed NoV concentrations in the static model (centered around 10^4 gc/L) were significantly lower than the concentrations estimated by the dynamic model—a difference of ~2 orders of magnitude when excluding secondary and foodborne transmission but up to ~4 orders of magnitude when all exposure routes were considered. When considering λ_1, λ_2, and λ_3, the NoV concentration in the raw wastewater was similar across all three potable reuse systems (median of ~10^8 gc/L), consistent with their similar CI values. When excluding secondary transmission ($\lambda_2 = 0$), the median pathogen load decreased to ~10^7 gc/L for all three systems, but when excluding foodborne transmission ($\lambda_3 = 0$), the effects were

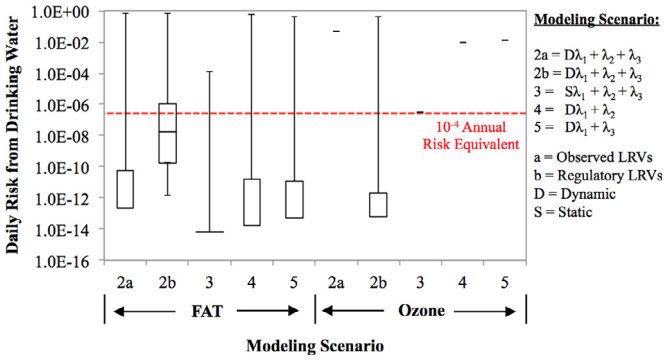

Fig. 8. Daily risk from drinking water (λ_1, d^{-1}) as a function of modeling scenario. Boxes represent 5th, 50th, and 95th percentiles, and whiskers indicate minimum and maximum values. For some scenarios, only the maximum risk was quantifiable by the model (i.e., >0). The dashed line corresponds with an annualized risk of 10^{-4}.

highly variable, which is consistent with the aforementioned oscillations in risk for scenario 4 (shown previously in Figs. 4 and S2). For *de facto* reuse, the median raw wastewater concentration in scenario 4 was ~10^7 gc/L, but for DPR, the model predicted concentrations as low as 0 gc/L and as high as ~10^{11} gc/L on a given day for FAT. The range was tighter for ozone-based treatment, and both systems exhibited a

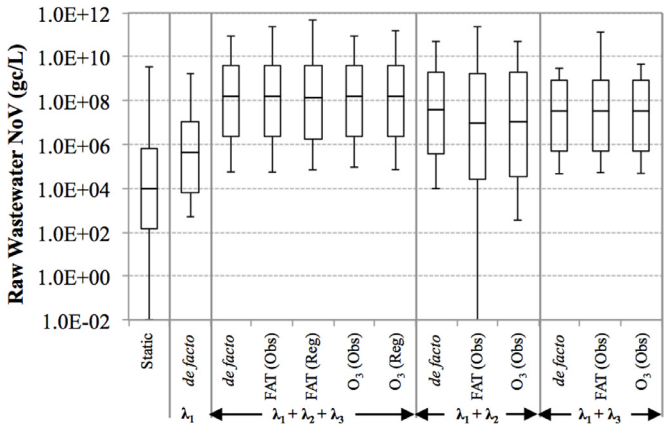

Fig. 9. Distribution of NoV concentrations in raw wastewater under static (lognormally distributed) and dynamic conditions (β_1, β_2, and/or β_3) and as a function of the log removal value framework (observed vs. regulatory). For the dynamic scenarios, the raw wastewater concentration was determined as the ratio of the daily pathogen load from infected individuals divided by the community's daily wastewater generation rate. Whiskers indicate minimum and maximum values, and boxes represent 5th, 50th, and 95th percentile values.

median concentration of $\sim 10^7$ gc/L.

Raw wastewater NoV concentrations have been a point of uncertainty in other QMRAs. For example, Amoueyan et al. (2019) assumed a mean of $\sim 10^{3.95}$ gc/L and Soller et al. (2018a) assumed a mean of $10^{4.70}$ gc/L. Both assumptions were based on the NoV review of Eftim et al. (2017), although Amoueyan et al. (2019) excluded seasonal effects and included data only from North America. Other occurrence studies reported raw wastewater NoV concentrations as high as $10^{7.5}$ gc/L for a single office building (Jahne, 2017) and $10^{7.7}$ gc/L for a single wastewater treatment plant affected by a seasonal spike in pathogen load (Simmons et al., 2011). It may be justifiable to use these high-end estimates of raw wastewater NoV concentrations for QMRAs considering that the model generated median concentrations ranging from 10^7–10^8 gc/L and maximum concentrations as high as 10^{11} gc/L in the community's raw sewage. However, the model did not account for any inactivation or physical removal that might occur in the sewer system. That could potentially reduce the peak concentrations predicted by the model, which would then cause them to align more closely with the estimates of Jahne (2017) and Simmons et al. (2011). Further study is needed to clarify the most appropriate concentrations to use for raw sewage and to quantify the expected level of inactivation in sewer systems.

4. Conclusion

The main goals of this study were to evaluate the performance of different potable reuse systems in the context of NoV risk and to compare the relative significance of primary (contaminated water and food) vs. secondary exposure, as this is rarely addressed in the QMRA literature. Consistent with real-world epidemiology, the results suggested that NoV infections were mainly attributable to secondary transmission and/or primary transmission via contaminated food. As long as the potable reuse system achieved the 10^{-4} annual risk benchmark, the drinking water had no discernible impact on overall risk. For *de facto* reuse, this was highly dependent on storage time in the environmental buffer. With a storage time of at least 15 days, the environmental buffer adequately attenuated the pathogen load to the system because of NoV's assumed rapid die-off kinetics. With a storage time of at least 30 days, the *de facto* reuse system was comparable or even superior to advanced treatment for DPR. Under normal operational conditions, both DPR treatment trains achieved the 10^{-4} annual risk benchmark, but compound failures combined with elevated NoV loads to the raw sewage resulted in short-term spikes in public health risk. It is important to note that such conditions are unlikely to occur because of the low probability of a catastrophic failure and the fact that DPR systems would likely require fail-safe protocols to mitigate or eliminate the impacts of a catastrophic failure. This highlights the robustness of advanced treatment trains typically employed for potable reuse but also underscores the importance of treatment process verification (e.g., by monitoring surrogate parameters at critical control points) to rapidly identify off-specification or failure conditions. Lastly, the elevated pathogen loads predicted by the dynamic model warrant further study to clarify whether elevated NoV concentrations should be assumed for QMRAs.

Declaration of Competing Interest

The authors declare no conflict of interest.

Acknowledgements

This publication was made possible by USEPA grant R835823: Early Career Award-Framework for Quantifying Microbial Risk and Sustainability of Potable Reuse Systems in the United States. Its contents are solely the responsibility of the grantee and do not necessarily represent the official views of the USEPA. Further, USEPA does not endorse the purchase of any commercial products or services mentioned in the publication. Graduate student funding was also provided by the UNLV Top Tier Doctoral Graduate Research Assistantship program. The authors would like to thank Dr. Joseph Eisenberg's epidemiology group at the University of Michigan and the reviewers for their valuable comments and suggestions.

Supplementary materials

Supplementary material associated with this article can be found, in the online version, at doi:10.1016/j.mran.2019.100088.

References

Amoueyan, E., Ahmad, S., Eisenberg, J.N., Pecson, B., Gerrity, D., 2017. Quantifying pathogen risks associated with potable reuse: a risk assessment case study for *Cryptosporidium*. Water Res.Res. 119, 252–266.

Amoueyan, E., Ahmad, S., Eisenberg, J.N., Gerrity, D., 2019. Equivalency of indirect and direct potable reuse paradigms based on a quantitative microbial risk assessment framework. Microb. Risk Anal. 12, 60–75.

Anderson, A.D., Heryford, A.G., Sarisky, J.P., Higgins, C., Monroe, S.S., Beard, R.S., Seys, S.A., 2003. A waterborne outbreak of Norwalk-like virus among snowmobilers—Wyoming, 2001. J. Inf. Dis. 187 (2), 303–306.

Aoki, Y., Suto, A., Mizuta, K., Ahiko, T., Osaka, K., Matsuzaki, Y., 2010. Duration of norovirus excretion and the longitudinal course of viral load in norovirus-infected elderly patients. J. Hosp. Infect. 75 (1), 42–46.

Atmar, R.L., Opekun, A.R., Gilger, M.A., Estes, M.K., Crawford, S.E., Neill, F.H., Graham, D.Y., 2008. Norwalk virus shedding after experimental human infection. Emerg. Infect. Dis. 14 (10), 1553–1557.

Barker, S.F., Packer, M., Scales, P.J., Gray, S., Snape, I., Hamilton, A.J., 2013. Pathogen reduction requirements for direct potable reuse in Antarctica: evaluating human health risks in small communities. Sci. Total Environ. 461, 723–733.

Boehm, A.B., Graham, K.E., Jennings, W.C., 2018. Can we swim yet? Systematic review, meta-analysis, and risk assessment of aging sewage in surface waters. Environ. Sci. Technol. 52, 9634–9645.

Brookhart, M.A., Hubbard, A.E., Van Der Laan, M.J., Colford, J.M., Eisenberg, J.N., 2002. Statistical estimation of parameters in a disease transmission model: analysis of a Cryptosporidium outbreak. Stat. Med. 21 (23), 3627–3638.

Brunkard, J.M., Ailes, E., Roberts, V.A., Hill, V., Hilborn, E.D., Craun, G.F., Carpenter, J., 2011. Surveillance for waterborne disease outbreaks associated with drinking water—United States, 2007–2008. MMWR Surveill. Summ. 60 (12), 38–68.

CDC, 2009. Surveillance for Foodborne Disease Outbreaks—United States, 2006 58. Centers for Disease Control and Prevention, pp. 609–615 MMWR Morbidity Mortality Weekly Report.

CDC, 2010. Surveillance for Foodborne Disease Outbreaks—United States, 2007 59. Centers for Disease Control and Prevention, pp. 973–979 MMWR Morbidity Mortality Weekly Report.

CDC, 2011. Surveillance for Foodborne Disease Outbreaks—United States, 2008 60. Centers for Disease Control and Prevention, pp. 1197–1202 MMWR Morbidity Mortality Weekly Report.

CDC, 2014. Vital Signs: Foodborne Norovirus Outbreaks—United States, 2009-2012. 63.

Centers for Disease Control and Prevention, pp. 491–495 MMWR Morbidity Mortality Weekly Report.
CDPH, 2014. Groundwater Replenishment Reuse Regulations. California Department of Public Health, Sacramento, CA.
Chaudhry, R.M., Hamilton, K.A., Haas, C.N., Nelson, K.L., 2017. Drivers of microbial risk for direct potable reuse and *de facto* reuse treatment schemes: The impacts of source water quality and blending. Int. J. Environ. Res. Public Health 14 (6), 635.
Currier, R.L., Payne, D.C., Staat, M.A., Selvarangan, R., Shirley, S.H., Halasa, N., Boom, J.A., Englund, J.A., Szilagyi, P.G., Harrison, C.J., Klein, E.J., Weinberg, G.A., Wikswo, M.E., Parashar, U., Vinjé, J., Morrow, A.L., 2015. Innate susceptibility to norovirus infections influenced by FUT2 genotype in a United States pediatric population. Clin. Infect. Dis. 60 (11), 1631–1638.
Eftim, S.E., Hong, T., Soller, J., Boehm, A., Warren, I., Ichida, A., Nappier, S.P., 2017. Occurrence of norovirus in raw sewage–a systematic literature review and meta-analysis. Water Res. 111, 366–374.
Eisenberg, J.N., Seto, E.Y., Olivieri, A.W., Spear, R.C., 1996. Quantifying water pathogen risk in an epidemiological framework. Risk Anal. 16 (4), 549–563.
Eisenberg, J.N., Seto, E.Y., Colford Jr, J.M., Olivieri, A., Spear, R.C., 1998. An analysis of the Milwaukee cryptosporidiosis outbreak based on a dynamic model of the infection process. Epidemiology 255–263.
Eisenberg, J.N., Brookhart, M.A., Rice, G., Brown, M., Colford Jr., J.M., 2002. Disease transmission models for public health decision making: Analysis of epidemic and endemic conditions caused by waterborne pathogens. Environ. Health Perspect. 110 (8), 783–790.
Eisenberg, J.N., Soller, J.A., Scott, J., Eisenberg, D.M., Colford Jr., J.M., 2004. A dynamic model to assess microbial health risks associated with beneficial uses of biosolids. Risk Anal. 24 (1), 221–236.
Eisenberg, J.N., Lei, X., Hubbard, A.H., Brookhart, M.A., Colford Jr, J.M., 2005. The role of disease transmission and conferred immunity in outbreaks: Analysis of the 1993 *Cryptosporidium* outbreak in Milwaukee. Wis. Am. J. Epidemiol. 161 (1), 62–72.
Forss, M., Ander, H., 2011. Microbiological Risk Assessment of the Water Reclamation Plant in Windhoek, Namibia. Thesis in the Master's Program Geo and Water Engineering. Department of Civil and Environmental Engineering. Chalmers University of Technology.
Gerrity, D., Pecson, B., Trussell, R.S., Trussell, R.R., 2013. Potable reuse treatment trains throughout the world. J. Water Supply Res. Technol. AQUA 62, 321–338.
Governal, R., Gerba, C., 1999. Removal of MS-2 and PRD-1 bacteriophages from an ultrapure water system. J. Ind. Microbiol. Biotechnol. 23 (3), 166–172.
Hall, A.J., Eisenbart, V.G., Etingue, A.L., Gould, L.H., Lopman, B.A., Parashar, U.D., 2012. Epidemiology of foodborne norovirus outbreaks, United States, 2001-2008. Emerg. Infect. Dis. 18 (10), 1566–1573.
Hall, A.J., Lopman, B.A., Payne, D.C., Patel, M.M., Gastañaduy, P.A., Vinjé, J., Parashar, U.D., 2013. Norovirus disease in the United States. Emerg. Infect. Dis. 19 (8), 1198–1205.
ILSI, 1996. A conceptual framework to assess the risks of human disease following exposure to pathogens. Risk Anal. 16, 841–848.
Jahne, M., 2017. Risk-Based Guidance for Decentralized Non-Potable Water Systems. USEPA. Office of Research and Development.
Johnson, P.C., Mathewson, J.J., DuPont, H.L., Greenberg, H.B., 1990. Multiple challenge study of host susceptibility to Norwalk gastroenteritis in US adults. J. Infect. Dis. 161, 18–21.
Karst, S.M., Zhu, S., Goodfellow, I.G., 2015. The molecular pathology of noroviruses. J. Pathol. 235, 206–216.
Lee, J., Zoh, K., Ko, G., 2008. Inactivation and UV disinfection of murine norovirus with TiO_2 under various environmental conditions. Appl. Environ. Microbiol. 74 (7), 2111–2117.
Lim, K., Wu, Y., Jiang, S.C., 2017. Assessment of *Cryptosporidium* and norovirus risk associated with *de facto* wastewater reuse in Trinity River. Tex. Microb. Risk Anal. 5, 15–24.
Lodder, W.J., de Roda Husman, A.M., 2005. Presence of noroviruses and other enteric viruses in sewage and surface waters in the Netherlands. Appl. Environ. Microbiol. 71 (3), 1453–1461.
Matsushita, T., Shirasaki, N., Tatsuki, Y., Matsui, Y., 2013. Investigating norovirus removal by microfiltration, ultrafiltration, and precoagulation–microfiltration processes using recombinant norovirus virus-like particles and real-time immuno-PCR. Water Res. 47 (15), 5819–5827.
Messner, M.J., Berger, P., Nappier, S.P., 2014. Fractional Poisson—a simple dose-response model for human norovirus. Risk Anal. 34 (10), 1820–1829.
Milbrath, M., Spicknall, I., Zelner, J., Moe, C., Eisenberg, J., 2013. Heterogeneity in norovirus shedding duration affects community risk. Epidemiol. Infect. 141 (8), 1572–1584.
NCHS, 2018. Final data for 2015. National vital statistics reports. Natl. Center Health Stat. 66 (1).
Nordgren, J., Sharma, S., Kambhampati, A., Lopman, B., Svensson, L., 2016. Innate resistance and susceptibility to norovirus infection. PLoS Pathog. 12 (4), e1005385.
Okhuysen, P.C., Jiang, X., Ye, L., Johnson, P.C., Estes, M.K., 1995. Viral shedding and faecal IgA response after Norwalk virus infection. J. Infect. Dis. 171, 566–569.
Olivieri, A., Eisenberg, D., Soller, J., Eisenberg, J., Cooper, R., Tchobanoglous, G., Gagliardo, P., 1999. Estimation of pathogen removal in an advanced water treatment facility using Monte Carlo simulation. Water Sci. Technol. 40 (4-5), 223–233.
Parshionikar, S.U., Willian-True, S., Fout, G.S., Robbins, D.E., Seys, S.A., Cassady, J.D., Harris, R., 2003. Waterborne outbreak of gastroenteritis associated with a norovirus. Appl. Environ. Microbiol. 69 (9), 5263–5268.
Pecson, B.M., Triolo, S.C., Olivieri, S., Chen, E.C., Pisarenko, A.N., Yang, C.C., Trussell, R.R., 2017. Reliability of pathogen control in direct potable reuse: Performance evaluation and QMRA of a full-scale 1 MGD advanced treatment train. Water Res. 122, 258–268.
Pecson, B.M., Chen, E.C., Triolo, S.C., Pisarenko, A.N., Olivieri, S., Idica, E., Kolakovsky, A., Trussell, R.S., Trussell, R.R., 2018. Mechanical reliability in potable reuse; evaluation of an advanced water purification facility. J. Am. Water Works Assoc. 110 (4), E19–E28.
Rao, S.S., 2006. Oral rehydration for viral gastroenteritis in adults: a randomized, controlled trial of 3 solutions. J. Parent. Enteral Nutr. 30, 433–439.
Regli, S., Rose, J.B., Haas, C.N., Gerba, C.P., 1991. Modeling the risk from *Giardia* and viruses in drinking water. J. Am. Water Works Assoc. 83 (11), 76–84.
Rice, J., Via, S.H., Westerhoff, P., 2015. Extent and impacts of unplanned wastewater reuse in U.S. rivers. J. Am. Water Works Assoc. 107 (11), E571–E581.
Sabria, A., Pinto, R.M., Bosch, A., Bartolome, R., Cornejo, T., Torner, N., Martinez, A., de Simon, M., Dominguez, A., Guix, S., 2016. Norovirus shedding among food and healthcare workers exposed to the virus in outbreak settings. J. Clin. Virol. 82, 119–125.
Salveson, A., Trussell, S., Macpherson, L., 2016. Guidelines for Engineered Storage for Direct Potable Reuse. Water Environment & Reuse Foundation Final report for WateReuse-12-06Alexandria, VA.
Scallan, E., Griffin, P.M., Angulo, F.J., Tauxe, R.V., Hoekstra, R.M., 2011. Foodborne illness acquired in the United States—unspecified agents. Emerg. Infect. Dis. 17, 16–22.
Simmons, F.J., Kuo, D.H., Xagoraraki, I., 2011. Removal of human enteric viruses by a full-scale membrane bioreactor during municipal wastewater processing. Water Res. 45 (9), 2739–2750.
Simmons, K., Gambhir, M., Leon, J., Lopman, B., 2013. Duration of immunity to norovirus gastroenteritis. Emerg. Infect. Dis. 19 (8), 1260–1267.
Soller, J.A., Eisenberg, J.N., 2008. An evaluation of parsimony for microbial risk assessment models. Environmetrics 19 (1), 61–78.
Soller, J.A., Eftim, S.E., Warren, I., Nappier, S.P., 2017. Evaluation of microbiological risks associated with direct potable reuse. Microb. Risk Anal. 5, 3–14.
Soller, J.A., Eftim, S.E., Nappier, S.P., 2018a. Direct potable reuse microbial risk assessment methodology: sensitivity analysis and application to State log credit allocations. Water Res. 128, 286–292.
Soller, J.A., Parker, A.M., Salveson, A., 2018b. Public health implications of short duration, off-specification conditions at potable reuse water treatment facilities. Environ. Sci. Technol. Lett. 5 (11), 675–680.
Sterman, J.D., 2000. Business Dynamics: Systems Thinking and Modeling for a Complex World. McGraw-Hill, New York, NY.
SWRCB (2016). Expert PANEL Final report: Evaluation of the feasibility of Developing Uniform Water Recycling Criteria for Direct Potable Reuse. State Water Resources Control Board. https://www.waterboards.ca.gov/drinking_water/certlic/drinkingwater/documents/rw_dpr_criteria/app_a_ep_rpt.pdf. Accessed: May 1, 2019.
Teunis, P., Sukhrie, F., Vennema, H., Bogerman, J., Beersma, M., Koopmans, M., 2015. Shedding of norovirus in symptomatic and asymptomatic infections. Epidemiol. Infect. 143 (8), 1710–1717.
Trussell, R.R., Salveson, A., Snyder, S., Trussell, R.S., Gerrity, D., 2016. Equivalency of Advanced Treatment Trains for Potable Reuse. Water Environment & Reuse Foundation Final report for WateReuse-11-02Alexandria, VA.
USEPA, 2002. Onsite Wastewater Treatment Systems Manual. EPA 625-R-00-008. United States Environmental Protection Agency, Washington, D.C.
USEPA, 2004. Estimated per capita water ingestion and body weight in the United States—An update. United States Environmental Protection Agency, Washington, D.C. EPA 822-R-00-001.
USEPA, 2006. National primary drinking water regulations: Long Term 2 Enhanced Surface Water Treatment Rule (LT2ESWTR); Final Rule. U.S. Environmental Protection Agency, Washington, D.C. EPA 815-Z-06-001.
USEPA, 2010. Long Term 2 Enhanced Surface Water Treatment Rule Toolbox Guidance Manual. U.S. Environmental Protection Agency, Washington, D.C. EPA 815-D-03-009.
WHO, 2008. Guidelines for Drinking-Water Quality. World Health Organization: Geneva, Switzerland.
Wu, Y., 2015. Quantitative Microbial Risk Assessment of *de facto* Water Reuse Practice: a Case Study of Trinity River, Texas. University of California, Irvine.
Zelner, J.L., King, A.A., Moe, C.L., Eisenberg, J.N., 2010. How infections propagate after point-source outbreaks: an analysis of secondary norovirus transmission. Epidemiology 21 (5), 711–718.
Zhang, S., Chen, T.H., Wang, J., Dong, C., Pan, J., Moe, C., Chen, W., Yang, L., Wang, X., Tang, H., Li, X., Liu, P., 2011. Symptomatic and asymptomatic infections of rotavirus, norovirus, and adenovirus among hospitalized children in Xi'an, China. J. Med. Virol. 83 (8) 1476-148.